JOURNAL OF CATALYSIS **132,** 388–401 (1991)

Microcalorimetric Study of Oxygen Adsorption on Catalytically Promoted Gasification Chars

A. S. GOW AND J. PHILLIPS[1]

Department of Chemical Engineering, The Pennsylvania State University, 133 Fenske Laboratory, University Park, Pennsylvania 16802-4400

Received July 19, 1990; revised June 27, 1991

The interaction between oxygen and the surface of raw and catalytically promoted (potassium or calcium) bituminous coal chars was studied using a novel true differential calorimeter. Results clearly indicated that on potassium-promoted chars, oxygen adsorbs onto a thin layer of partially oxidized potassium. Also the oxygen uptake on potassium-promoted chars was found to be much greater than on calcium or unpromoted chars. This supports the view that potassium "spreads" on char surfaces. In contrast, these calorimetric results and the results of parallel XRD studies suggest that on demineralized bituminous coal calcium sinters and alloys with residual sulfur to produce relatively inactive catalysts. These findings strongly support one earlier model of potassium-promoted coal char reactivity: potassium catalyzes char gasification through a process in which a thin partially oxidized potassium film is alternately oxidized by the gas and reduced by the char.

INTRODUCTION

Catalytic gasification of carbonaceous materials continues to be an industrially important process; the past decade has witnessed a flurry of research activity in all phases of catalytic carbon gasification. Excellent reviews of this progress are available (*1–3*). Yet, particularly in the cases of alkali and alkaline-earth metal-catalyzed gasification of coal chars, there is considerable debate as to the mechanism of gasification and identification of the catalytically active phase. One model of metal-enhanced coal char reactivity, the so-called oxygen transfer mechanism, is that (i) gas adsorption takes place upon the metal or carbon-adsorbing sites, (ii) the gas is activated, and (iii) the activated gas atoms diffuse to where reaction takes place (*2, 4–7*). This can involve an oxidation/reduction cycle of the metal (*8–10*). One major unanswered question from this model is that regarding the path of activated oxygen diffusion (*3, 11*). Another question relates to the state of the metal. For example, potassium has been described both as metallic (*5, 11*) and partially oxidized (*8–10, 12*). To properly evaluate the above models of reactivity for catalyzed chars it is necessary to obtain accurate information regarding the number and identity of both carbon and catalyst sites.

Adsorption methods previously used to characterize chars include N_2 and CO_2 adsorption for total surface area (*13–15*), O_2 chemisorption, and various desorption studies for determination of catalytic site concentration (*6, 16, 17*). No combination of these methods is able to provide detailed information about the chemical structure of the catalytic surface. For example, oxygen chemisorption on metal-impregnated surfaces is currently the best method available for obtaining an approximate value for the total catalytic surface area. Yet, it is impossible to distinguish metal catalytic surface from active carbon surface using this method. It is also impossible to get quantitative data on the phase (e.g., oxidation state) of the various catalytic metals. The present study was designed to demonstrate that a

---

[1] To whom correspondence should be addressed.

0021-9517/91 $3.00

true differential calorimeter can yield quantitative data regarding the number and identity of oxygen-adsorbing sites on both raw and catalytically promoted (K and Ca) chars.

On the basis of these studies several conclusions were reached. With regard to demineralized uncatalyzed bituminous coal chars it is felt, in agreement with earlier workers (*15–18*), that the gas-adsorbing sites are chemically similar to those found on high-surface-area carbons. With regard to chars prepared with $CaCO_3$ (alkaline-earth metal salt) it was found that the calcium salt, following either high-temperature or low-temperature preparation, did not significantly change the amount of oxygen adsorbing surface. These chars have an active site population similar to that of the raw chars. In contrast, the addition of K_2CO_3 to the demineralized bituminous coal and subsequent charring had a dramatic effect. It increased the number of adsorbing sites and changed the rate and heat of oxygen adsorption. Also, the observed heats of adsorption clearly suggest the catalytically active surface in potassium carbonate-catalyzed gasification is partially oxidized potassium. This finding supports the oxidation–reduction mechanism of char gasification in which partially oxidized potassium present in thin layers is the active phase. The results also suggest a "path" for activated oxygen diffusion.

EXPERIMENTAL

Calorimeter. The design and operation of the Calvet-type calorimeter used in this work is described in detail elsewhere (*19, 20*). The reliability of the technique is affirmed by the results of previous studies in this laboratory (*21, 22*). The procedure is described briefly below. The sample is exposed to a measured amount of gas in a thermally controlled environment at 303 K. Heat generated by the adsorption of the gas flows out of the sample chamber through thermopiles, which generate a signal proportional to the instantaneous heat flow. The integrated signal is proportional to the total heat generated. The shape of the heat peaks yield qualitative information regarding the kinetics of the adsorption process. Once the system has returned to equilibrium the procedure is repeated. This is done repeatedly until it is clear from the signal shape and strength that very little heat is being produced and that the gas is only physically adsorbing on the sample.

Note that the temperature of adsorption (303 K) is lower than the temperature conventionally used to titrate carbon active sites with oxygen (*23*), although temperatures as low as 375 K have been used (*13*). One advantage of performing the adsorption at a low temperature is that the only process that takes place is the adsorption of oxygen. There are no simultaneous processes that lead to product desorption as have been encountered in higher-temperature studies of oxygen/carbon interaction (*24*). Thus, the results reported are not ideal for comparison with active surface area (ASA) studies, but are excellent for comparison with earlier calorimetric studies of oxygen adsorption on carbon (*20, 25–27*), and for contrast with adsorption on chars containing catalyst.

BET and Polyani–Dubinin (P-D) measurements. The BET and P-D (CO_2) measurements were conducted in a standard glass high-vacuum system with an ultimate pressure of 1×10^{-6} Torr. After char production, described below, each of these samples was exposed to the ambient laboratory atmosphere for several days before surface area measurements were conducted. The procedures used in making the surface area measurements are standard and are described in detail elsewhere (*15*).

X-ray diffraction. XRD characterization of the samples was conducted in air using a Rigaku Model DMAX-IA diffractometer. This diffractometer employs a copper target X-ray source, curved crystal graphite monochrometer, and Ti-drifted NaI scintillation detectors. The distance between sample and detector is 185 mm and a divergent slit of 1° and a receiving slit of 0.3° were used.

Sample preparation. Experiments were conducted on samples from the same batch of bituminous coal char (Pitt No. 8, sample No. MQA1; received from the DOE/PSU Coal Bank). Demineralization was carried out, using the method of Bishop and Ward (*28*), as follows. (1) Six grams of coal, ground under nitrogen to pass 200 mesh, were mixed with 40 ml of 5 *N* HCl in a plastic beaker (125 ml). The slurry was then agitated at 60°C for 1 h. (2) The coal was filtered, washed, and bathed in stirred full-strength HF at 60°C for 1 h. (3) Step (2) was repeated except with full-strength HCl. (4) The coal was then filtered and continuously washed with distilled water. (5) A slurry was prepared with an excess of CO_2-free distilled water and refluxed for several hours. It was necessary to repeat step (4) until no chlorine was detected in the filtrate with an indicator. The coal was thoroughly dried in air at 50°C for 24 h.

Altogether six samples were studied: (i) char prepared by devolitilization of the parent coal at 500°C, (ii) char prepared by devolitilization of the parent coal at 900°C, (iii, iv) chars prepared by physically mixing the demineralized parent coal with metal carbonate (K_2CO_3 or $CaCO_3$) and then devolitilizing at 500°C, and (v, vi) chars prepared by physically mixing the demineralized parent coal and metal carbonates and then devolitilizing at 900°C. Relevant parameters for each sample are given in Table 1. More detail on sample preparation is given below.

In order to accommodate the inherent physical limitations of the calorimeter all of the coal underwent a three-stage treatment before measurements were made. That is, the coal was first pyrolyzed, then crushed, and finally heat treated. This sequence was chosen since high-rank low-volatile coals form a plasticized material upon cooling (*29*). The exact procedure for the two "raw" samples is described below. The same procedure was carried out for the "loaded" samples except in these cases 10% by weight of a fine powder of calcium or potassium carbonate was physically mixed into the coal before any heat treatments.

TABLE 1

Sample Preparation Specification

Sample	Added by physical mixing	Pyrolysis conditions	Offgassing treatment
Low-temperature raw	No catalyst	1 h–500°C flowing N_2, crushed	3 h–500°C, 1×10^{-4} Torr
High-temperature raw	No catalyst	1 h–500°C flowing N_2, crushed	3 h–900°C, 1×10^{-4} Torr
Low-temperature calcium	$CaCO_3$	1 h–500°C flowing N_2, crushed	3 h–500°C, 1×10^{-4} Torr
High-temperature calcium	$CaCO_3$	1 h–500°C flowing N_2, crushed	3 h–900°C, 1×10^{-4} Torr
Low-temperature potassium	K_2CO_3	1 h–500°C flowing N_2, crushed	3 h–500°C, 1×10^{-4} Torr
High-temperature potassium	K_2CO_3	1 h–500°C flowing N_2, crushed	3 h–900°C, 1×10^{-4} Torr

Demineralized raw coal was heated under flowing N_2 in a tube furnace to 500°C, held at that temperature for 1 h, and then cooled gradually (ca. one-half hour) to room temperature. This process resulted in the formation of an agglomerated/plasticized material. This material was crushed to a fine powder using a mortar and pestle. From this powder two samples were made. A "high-temperature" sample was prepared by heating the powder (1.5 h) to 900°C in a vacuum furnace (1×10^{-4} Torr), holding it there for 3 h, then cooling it gradually (1.5 h) to room temperature. The sample was held under dynamic vacuum for an additional 10 h before being vacuum transferred into the calorimeter sample cell. A "low-temperature" sample was prepared in a nearly identical manner, however, this sample was heated only to 500°C.

Catalysts were added by the process of physically mixing metal carbonates with the demineralized coal prior to preparation. This method was used since prior studies (*2, 30*) have indicated that this will leave highly

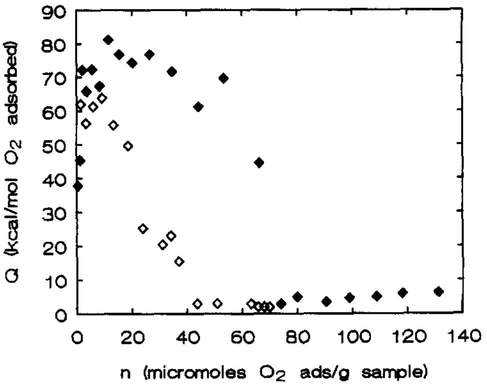

FIG. 1. Differential heat of oxygen adsorption versus the quantity of gas adsorbed for the 500°C (◇) and 900°C (◆) offgassed chars. The low-temperature-treated char clearly chemisorbs less gas than its high-temperature-treated counterpart.

dispersed catalyst particles on the coal char in certain cases (e.g., potassium carbonate) and poorly dispersed particles in others (e.g., calcium carbonate). Some insight regarding this contrasting behavior was desired here.

RESULTS

Oxygen adsorption on raw demineralized chars. Figure 1 shows the differential heat of adsorption vs the amount adsorbed per gram of sample for both the low- and high-temperature raw chars. The adsorption process on the two samples is clearly different. The differential heat vs coverage fluctuates for both samples; however, the initial adsorption occurs at a much lower heat (ca. 40 kcal/mol) for the 900°C treated sample than for the 500°C sample (ca. 65 kcal/mol). Also, the differential heat of adsorption achieved a maximum of over 80 kcal/mol for the high-temperature-treated sample, whereas the heat only climbed to about 65 kcal/mol for the low-temperature-treated sample. Moreover, the high-temperature-treated char clearly adsorbed more gas.

There is also qualitative information available regarding the kinetics of the adsorption process. In Fig. 2, normalized cooling width (NCWHM) is plotted on the same figure as the heat of adsorption. The normalized cooling width is the time elapsed from the moment at which the maximum in the heat output curve is reached until the half height point, normalized relative to the cooling width of the first heat output curve of that sample. Initially on both samples the adsorption process is relatively rapid. With each subsequent dose, however, heat production and hence output takes longer. This indicates that the chemisorption process (Region I) takes progressively longer to complete. Eventually, only physical adsorption (Region II) takes place, and heat output becomes very rapid.

It is notable that both the heats and kinetics of oxygen adsorption observed for these raw char samples is similar to that observed on some high surface area carbons (*19, 20, 25–27*).

The fact that the differential heat increases or fluctuates (Region I) is not thought to be instrument error because of the smoothness of the raw data; the steady change of the NCWHM; the repeatability of the chaotic behavior on several samples; the contrast with the steady decline in heat observed with other samples in this study; and previous experience with a similar calorimeter (*20*). It must be emphasized that if an adsorption process is kinetically controlled, there is no theoretical reason for the ΔH values to decrease smoothly. It is also expected that adsorption on a heterogeneous surface, such as that presented by coal char, will be controlled by kinetics, not equilibrium. Moreover, the suggestion that the adsorption process is kinetically controlled on these samples is consistent with the NCWHM data, which show adsorption to slow with each dose (*20, 31*).

Oxygen adsorption on $CaCO_3$-loaded chars. Figures 3a and 3b show the heat of adsorption and NCWHM data for the low- and high-temperature $CaCO_3$ loaded char respectively. There are both similarities and differences between the heats and kinetics

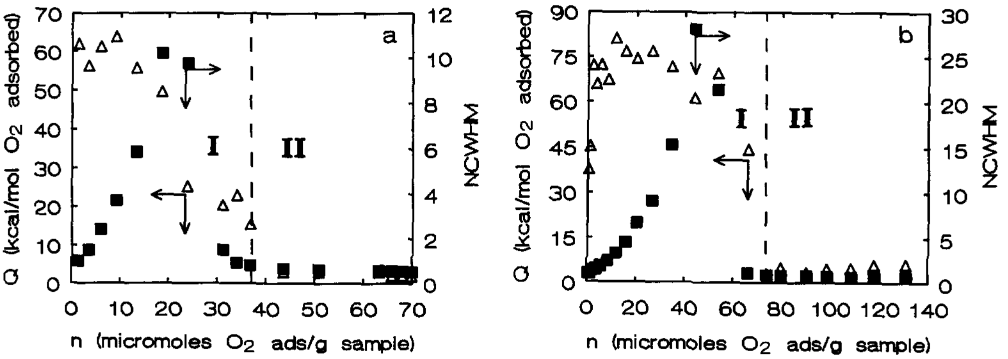

FIG. 2. Calorimetric study of raw chars. (a) Differential heat of oxygen adsorption (△) and NCWHM (■) versus the quantity of gas adsorbed for the 500°C raw pretreated char. The marked regions are discussed in the text. (b) Differential heat of oxygen adsorption (△) and NCWHM (■) versus the quantity of gas adsorbed for the 900°C raw pretreated char.

of adsorption on these samples and those on the raw char samples. The principle similarities are that the total amount chemically adsorbed is similar and the kinetics and heats of adsorption are not dramatically different. The principle differences are that, except for the first two/three doses, the heats decrease smoothly on the calcium-promoted chars, and more gas adsorbs after the low-temperature treatment than after the high-temperature treatment.

Region I behavior for adsorption of oxygen on the two calcium chars is somewhat different in each case. The heats follow a smooth trend for both samples; however, they drop off far more rapidly for the high-temperature char. Moreover, as in the raw char case the maximum value for the parameters NCWHM for the high-temperature char is much greater than that for the low-temperature sample.

Oxygen adsorption on K_2CO_3-loaded chars. The heat vs amount adsorbed data is clearly different for these samples (Figs. 4a and 4b), than that obtained for raw chars and calcite loaded chars. Following is a list of the chief differences. (i) The heats of adsorption are distinctly different than on raw

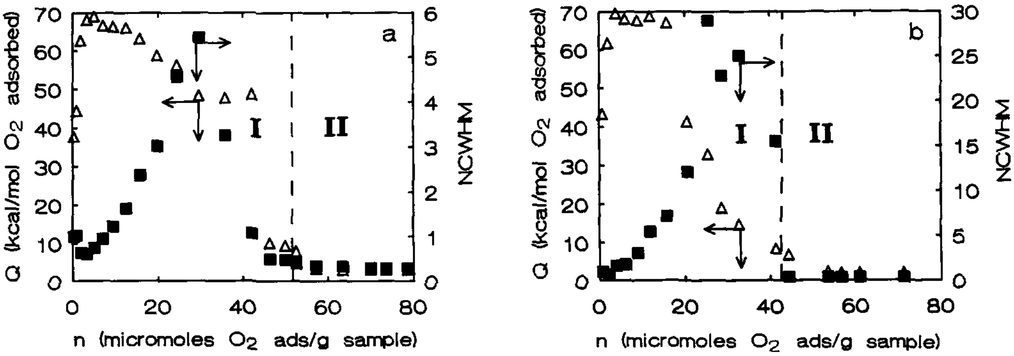

FIG. 3. Calorimetric study of calcium-loaded chars. (a) Differential heat of oxygen adsorption (△) and NCWHM (■) versus the quantity of gas adsorbed for the 500°C $CaCO_3$ pretreated char. (b) Differential heats of oxygen adsorption (△) and NCWHM (■) versus the quantity of gas adsorbed for the 900°C $CaCO_3$ pretreated char.

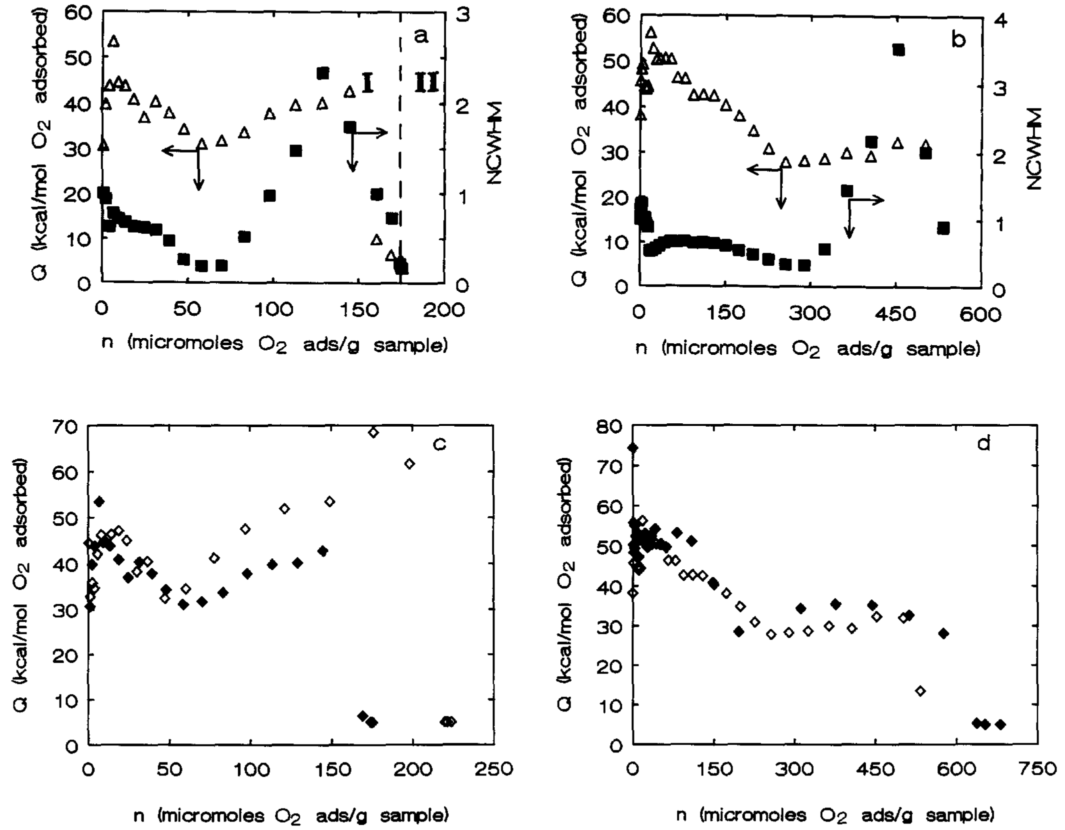

FIG. 4. Calorimetric study of potassium-loaded chars. (a) Differential heats of oxygen adsorption (△) and NCWHM (■) versus the quantity of gas adsorbed for the 500°C K_2CO_3 pretreated sample. (b) Differential heats of oxygen adsorption (△) and NCWHM (■) versus the quantity of gas adsorbed for the 900°C K_2CO_3 pretreated char. This char chemisorbs by far the most gas of any of the six samples. (c) Differential heat of oxygen adsorption versus the quantity of gas adsorbed for the low-temperature-pretreated K_2CO_3 char. The two experiments show that the data are fairly reproducible. See text for details. (d) Differential heat of oxygen adsorption versus the quantity of gas adsorbed for the high-temperature-pretreated K_2CO_3 char. The data for two experiments indicate good reproducibility.

chars or carbons. On both low- and high-temperature chars the heats are between 30 and 50 kcal/g mol O_2 adsorbed over a wide range of coverage. These numbers are distinctly lower than those on the other samples. (ii) The rate of chemisorption is steady over a broad range of coverages, particularly on the high-temperature sample. (iii) Nearly an order of magnitude more gas is absorbed on these samples than on the other samples. (iv) Finally, the temperature of the pretreatment makes a significant difference in the number of adsorbing sites. This is not the case for the other samples.

Second trials with fresh samples show that the data is reproducible to a fairly high degree. That is, an analysis of the differential heat spectra for two low-temperature samples (Fig. 4c) indicates that the data follow the same basic trend with only a minor discrepancy in heats at moderate to high coverage. Moreover, both samples chemisorb nearly the same amount of gas. Similar behavior is observed for the high-temperature samples (Fig. 4d).

Adsorption isotherms and Surface Area estimates. Operation of the calorimeter also produces equilibrium adsorption data; that

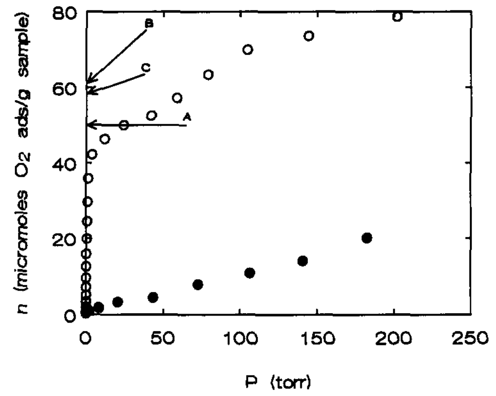

FIG. 5. Isotherms of oxygen adsorption on the 500°C $CaCO_3$ pretreated char. These isotherms (type I) are typical of those seen on all six samples studied (○). The total quantity of gas chemisorbed on the chars was determined in three ways as discussed in the text. The three methods yielded similar results for all six coal chars. The total amount of gas chemisorbed was used to calculate the catalyst surface area corresponding to each method for all chars by assuming that an adsorbed oxygen molecule occupied 20 Å^2 on the char surface. These results are summarized in Table 2. The second isotherm (●) was obtained after 1 h of pumping.

is, the final (pseudo-equilibrium) pressure vs cumulative amount adsorbed is obtained for each dose. This information can be used to generate conventional isotherms.

Figure 5 shows adsorption isotherms for the low-temperature $CaCO_3$-loaded sample. Three methods were used to determine the oxygen adsorption capacity at 303 K. The letter A (left axis, Fig. 5) indicates the amount of chemisorbing surface area measured on the basis of the heat of adsorption data (ΔH greater than 10 kcal/g mol adsorbed). The letter B indicates the capacity measured on the basis of a single isotherm, and C indicates the amount of chemisorbing gas measured on the basis of the two isotherm methods. All three methods give the same value within a factor of about 1.5 for all samples, which is very good agreement (Table 2). However, the isotherm data, which are typically the only data available, do not provide any information regarding possible distribution of chemisorbing sites, the strength, or the kinetics of adsorption at these sites.

TABLE 2

Total Oxygen Uptake

Sample	O_2 uptake from heats ($\Delta H > 10$ kcal/mol) (m^2/g)	Single isotherm total O_2 uptake (m^2/g)	Dual isotherm total O_2 uptake (m^2/g)
500°C Raw	5.1	7.0	6.6
900°C Raw	8.9	10.2	10.2
500°C $CaCO_3$	5.8	7.2	7.0
900°C $CaCO_3$	4.6	5.4	5.5
500°C K_2CO_3	36.1	29.5	28.9
900°C K_2CO_3	66.3	63.6	60.2

BET and P-D surface area estimates. Values of BET and P-D surface area for all six chars are given in Table 3. The BET measurements indicate that all of the chars have little or no mezo- or macro-pore surface area; however, the P-D surface areas indicate that the raw chars and the calcite-promoted chars have a high micropore surface area. In contrast, the potassium-promoted chars have a far smaller micropore surface area. In fact, the oxygen-adsorbing capacity for the high-temperature potassium-promoted char is apparently higher than the total micropore surface area.

X-ray diffraction analysis. Results of the XRD study of five of the six post-calorimetric air-exposed samples are presented in Figs. 6–8. The diffraction pattern for the raw 900°C sample is not shown because it is identical to that for the low-temperature sample. Reflections from the Grafoil sample

TABLE 3

Surface Areas of Coal Chars

Sample	BET (m^2/g)	P-D (m^2/g)
500°C Raw	7.7	289
900°C Raw	1.4	289
500°C $CaCO_3$	14.0	250
900°C $CaCO_3$	3.2	206
500°C K_2CO_3	6.6	77
900°C K_2CO_3	1.6	13

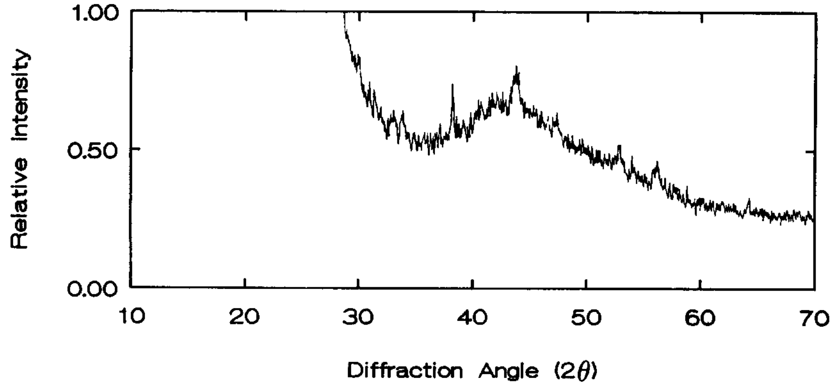

FIG. 6. XRD study of raw chars. XRD pattern of 500°C raw pretreated sample following calorimetric oxidation and subsequent air exposure. All strong peaks observed for this sample and the high-temperature raw sample are explained by the Grafoil sample holder.

holder are found at 13°, 25°, and 54° (*32*) and act as an internal standard. It should be noted that the data in this study are for identification of the final oxidized state of the catalyst-char system.

Figure 6 depicts the diffraction pattern for the raw demineralized char pretreated at 500°C. Note that no strong peaks are present other than those attributable to the holder. Hence, it is likely that the demineralization has removed much of the mineral matter from the coal and that any residual material is well dispersed.

Diffraction patterns for the $CaCO_3$-treated chars are shown in Figs. 7a and 7b. All of the additional peaks observed for the low-temperature char (Fig. 7a) are explained by the presence of $CaCO_3$, suggesting that at 500°C, $CaCO_3$ does not decompose. This is borne out by thermodynamic calculations that predict a decomposition pressure of 4.5×10^{-5} Torr at a temperature of 500°C. In the diffraction pattern of the high-temperature char (Fig. 7b) the peaks at 31.2°, 44.7°, and 55.5° are identified as calcium sulfide (CaS), while the peaks at 32.2°, 37.4°, 53.8°, and 64.1° are identified as calcium oxide (CaO). The peaks at 17.8°, 33.8°, 47.0°, and 50.5° are attributed to $Ca(OH)_2$. This is consistent with past observations that bituminous coals contain a considerable amount of pyrite (FeS) (cannot be removed via demineralization) with which the CaO produced (from high-temperature decomposition of the calcite) readily reacts to form CaS. Some of the excess CaO then picks up atmospheric water to form $Ca(OH)_2$.

The diffraction patterns for the potassium-catalyzed samples are given in Figs. 8a and 8b. Note the appearance of several distinct nongraphitic peaks in the XRD pattern for the low-temperature sample. Apparently all of the K_2CO_3 is chemically converted to a mixture of potassium oxides, as evidenced by the appearance of a band of several peaks around 30° (Fig. 8a), all of which could result from various potassium oxides (e.g., K_2O and KO_2). XRD clearly indicates that no K_2CO_3 remains following heat treatment and subsequent air exposure. However, the diffraction pattern suggests that following the high-temperature treatment (Fig. 9b) the potassium has a less-well-defined crystallinity as evidenced by the disappearance of most peaks.

DISCUSSION

The data collected in this work permit clear contrasts between the low-temperature (300 K) oxygen-adsorbing sites on each of the different surfaces. The data can also

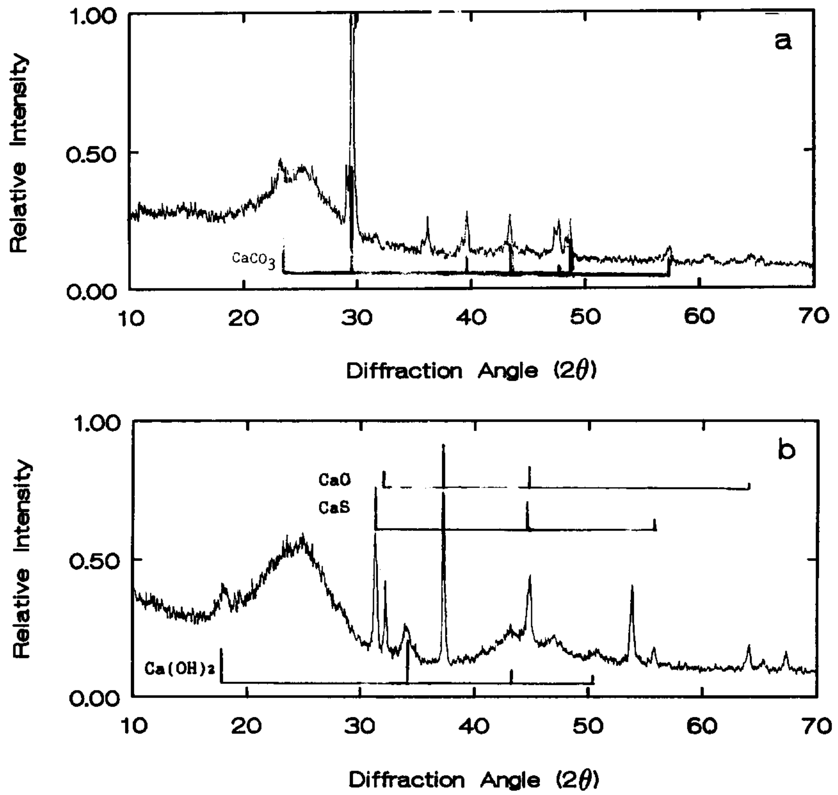

FIG. 7. XRD study of calcium-loaded chars. (a) XRD pattern of 500°C $CaCO_3$ pretreated sample following calorimetric oxidation and subsequent air exposure. All nongraphitic peaks are due to the presence of a bulk carbonate phase. (b) XRD pattern of 900°C $CaCO_3$ pretreated sample following calorimetric oxidation and subsequent air exposure. It is evident that calcium sulfide, calcium oxide, and calcium hydroxide are present.

be correlated to previously observed differences in reactivity permitting, particularly in the case of potassium promoted chars, an improved understanding of the catalytic mechanism.

Raw chars. A simple model of the chemistry of raw coal chars can be developed on the basis of the calorimetric studies. Specifically: The gas-adsorbing sites on the raw char are similar to those found on high surface area carbons. There are a variety of adsorbing sites that are not in chemical contact (heterogeneous surface), such that the adsorption process is controlled by kinetics and not equilibrium considerations. Finally, high-temperature pretreatments increase the number of oxygen adsorbing sites (at 300 K) by desorbing site-blocking species from the char surface.

Previous studies of adsorption of oxygen on high surface area carbons support the first claim. Several groups have shown that the heats of adsorption of oxygen on "clean" carbon surfaces yield initial heats of around 70 kcal/g mol (*20, 25–27*), which gradually decrease. This is similar to the heats observed in this study. It has also been shown that the adsorption process on carbons is generally kinetically controlled (*20, 31*). In fact, for studies of carbon total active surface area (ASA) higher adsorption temperatures are employed specifically to overcome kinetic barriers (*23, 33*).

One plausible explanation for the fluctua-

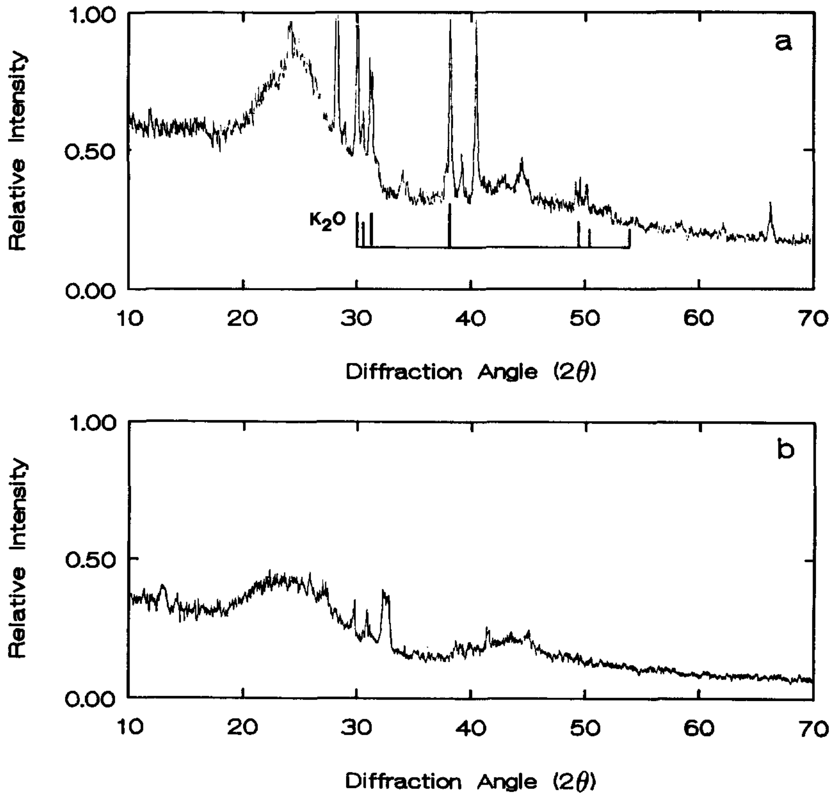

FIG. 8. XRD of potassium-loaded chars. (a) XRD pattern of 500°C K_2CO_3 pretreated sample following calorimetric oxidation and subsequent air exposure. This figure suggests that a mixture of potassium oxides is present. (b) XRD pattern of 900°C K_2CO_3 pretreated sample following calorimetric oxidation and subsequent air exposure. There are no clearly identifiable species.

tions in the heats of adsorption is that the surface is a heterogeneous one such that kinetics controls the adsorption process. A thorough discussion of this is not merited in the present context, but is available elsewhere (*21, 30*). A few standard concerns are addressed here. For example, if diffusion into the bed or individual particles were rate controlling, then equal heats of adsorption would be found for each dose, as pointed out in several places (*34, 35*). Moreover, there would be a constant decrease in the rate of adsorption. Also, physical adsorption, experimentally found to be the most rapid, would be the slowest process as equilibrium of physical adsorption would not be obtained until gas had diffused to all parts of the sample surface. In sum, a model in which diffusion controls the adsorption process is not consistent with the data.

Calcium carbonate-loaded chars. It is clear that there are only subtle differences in the character of oxygen adsorption between the raw chars and the calcium-loaded chars. The major difference is that over a wide range of coverage there are no fluctuations in the heat of adsorption on calcium-loaded chars. The similarities suggest that the calcium does not create a large number of new gas-adsorbing sites. Possibly adsorption on these chars occurs both on the surfaces of large "calcium" particles and on carbon sites. Competition between site types could explain the initial fluctuations.

The conclusion that calcium is not creating a significant number of new catalyst sites is consistent with the X-ray studies. For example, it is clear that on the low-temperature sample most of the $CaCO_3$ is not fully decomposed and is present as poorly dispersed particles. The high-temperature treatment converts a great deal of the calcium to calcium sulfide. The remainder is probably present as poorly dispersed CaO. It is also noteworthy that the surface areas (BET and P-D) are similar for the raw chars and calcium-loaded chars.

This model of calcium behavior is consistent with earlier studies. For example, adding calcium to coal chars is a well-known method for reducing sulfur emissions. It has been shown that this results from the interaction of calcium and sulfur to form stable compounds (*36*). It has also been found that the method of addition and pyrolysis history strongly influence dispersion in calcium salt catalyzed char system (*2, 37*). In particular, it is well known that high dispersions of calcium can only be achieved by ion exchange or by other chemical methods and only on some chars. Physical mixing does not work. Moreover, calcium looses activity and sinters at high temperatures into large particles of CaO, no matter what the initial dispersion (*37, 38*). It has also been shown that calcium must be added in rather large quantities to significantly increase reactive site density and activity per unit area (*39*).

Potassium carbonate-loaded chars. Given all the data a model of the morphology of the potassium layer and its oxidation state, particularly following the high-temperature treatment, can be developed. The model developed is similar to that developed using other techniques.

The morphology of the surface layer is a very thin (a few atomic layers) skin of a potassium-based structure. The adsorption sites on the potassium chars are probably nearly all associated with the promoter and not carbon sites. The dramatic increase in the amount adsorbed could be linked to the creation of new carbon sites, but this seems unlikely as the heats of adsorption on both samples are too low to be explained in that fashion. This suggestion that potassium carbonate creates many new oxygen-adsorbing sites is consistent with earlier models of potassium behavior on chars. It has been shown that potassium "melts" or "spreads" to form a thin film on carbon during heating at high temperatures (*41*).

Area measurements (BET, P-D) support the contention that the potassium layer is very thin. That is, the oxygen-adsorbing area is about equal to the total surface area for the low-temperature sample and is larger than the total surface area for the high-temperature sample. Also, the total surface area on both samples is considerably less than that on the other char samples. These findings suggest (i) the potassium spreads to form a thin layer, which virtually covers the entire surface, (ii) the spreading potassium blocks many pores, significantly reducing the total surface area, and (iii) oxygen adsorption is not confined simply to the very surface layer. The first two suggestions are consistent with earlier models of potassium behavior (*40, 41*). The third point is consistent with other studies of oxygen adsorption on metals. For example, it has been shown that iron that is differentially dosed with oxygen at room temperature will passivate only following the formation of two or three layers of oxide (*21*). This suggests that the potassium oxide layer is actually several atomic layers thick.

The impact of preparation temperature on oxygen uptake also provides an indirect indication of the thickness of the catalyst layer. If it is assumed that all potassium is in the form of K_2O following pretreatment (see later discussion) and that only KO_2 is formed by interaction with oxygen, then the fraction of K_2O oxidized during the calorimetric experiment can be determined. Results from all four potassium-promoted samples are listed in Table 4. These results clearly indicate that preparation temperature plays a dramatic role in catalyst dispersion on potassium-promoted samples. The oxide film is likely less dispersed on low-

TABLE 4

Oxide Film Dispersion on Potassium Carbonate-Promoted Chars

Sample	Wt% K	% K_2O oxidized to KO_2[a]
500°C	6.6	13
500°C (rerun)	6.9	15
900°C	5.3	52
900°C (rerun)	5.8	55

[a] See text for explanation of assumptions employed.

temperature-treated samples as supported by 13 and 15% K_2O oxidized as compared to 52 and 55% K_2O oxidized for the high-temperature-treated samples. (Note that the latter values are corrected for evaporation. See Table 4.) These results show that it is plausible that a significant amount of potassium is already partially oxidized prior to gas adsorption and that it is present in very thin layers. These results and the fact that the heats of adsorption are similar following both low- and high-temperature treatment also suggest that the spreading has not fully developed after treatment at 500 C.

Next, the question of oxidation state arises. If potassium metal is produced during heat treatment, then subsequent oxidation would occur as one or more of the following reactions:

$$\tfrac{4}{3}\,K\,(s) + O_2\,(g) \rightarrow \tfrac{2}{3}\,K_2O_3\,(s) \qquad \Delta H = -85.2 \text{ kcal/mol } O_2 \quad (1)$$

$$K\,(s) + O_2\,(g) \rightarrow KO_2\,(s) \qquad \Delta H = -68.4 \text{ kcal/mol } O_2 \quad (2)$$

and

$$2\,K\,(s) + O_2\,(g) \rightarrow K_2O_2 \qquad \Delta H = -118.3 \text{ kcal/mol } O_2 \quad (3)$$

Other potential reactions include

$$4\,K\,(s) + O_2\,(g) \rightarrow 2\,K_2O \qquad \Delta H = -172.8 \text{ kcal/mol } O_2 \quad (4)$$

and

$$\tfrac{2}{3}\,K\,(s) + O_2\,(g) \rightarrow \tfrac{2}{3}\,KO_3 \qquad \Delta H = -42.2 \text{ kcal/mol } O_2. \quad (5)$$

Reactions (1)–(5) do not seem likely since the heats of oxidation are generally outside the range of the observed heats. Alternately, the potassium may be already partially oxidized, due to decomposition of the carbonate, and in the form K_2O_{1-x}. Initially enough oxygen would be adsorbed to make stoichiometric crystals. Next, additional oxygen would be adsorbed, as per the following reaction:

$$K_2O + \tfrac{3}{2}\,O_2 \rightarrow 2KO_2 \qquad \Delta H = -34 \text{ Kcal/g mol } O_2. \quad (6)$$

The value of ΔH for this reaction is close to that observed experimentally.

X-ray studies, conducted after air exposure, are consistent with but do not prove the suggestion that the final stable forms of the potassium are partially oxidized thin films. Indeed, the loss of detectable crystal structure following high-temperature treatments is consistent with thin layer formation. Also, the X-ray results allow alternative explanations to be rejected. One suggestion (*42*) is that at low K_2CO_3 loadings a substantial amount of the catalyst formed during pyrolysis interacts with the mineral matter in the coal to form potassium aluminosilicates. None of the potassium aluminosilicates listed in the powder diffraction files were found to be present in the bulk. A second theory has the potassium catalyst interacting with the graphitic carbon in the char to form intercalate-like structures. Kapteijn *et al.* (*43*) have found this to be the case for one high-rank K_2CO_3-catalyzed gasification char. None of the patterns presented in earlier studies can explain the peaks in Figs. 8a or 8b. Thus, it seems unlikely that an intercalated potassium structure has formed.

Mims and Pabst (*12, 44*) suggested that potassium–oxygen–carbon complexes form on the char surface and are responsible for the excellent dispersion and reactivity of K_2CO_3-catalyzed chars. This is impossible to substantiate using XRD. However, if it is true that the potassium carbonate decomposes and forms surface phenoxide groups during pyrolysis as suggested by Mims and Pabst (*12*), then the nature or type of these groups present on the surface should be a strong function of temperature. Indeed, there is a dramatic contrast between the behavior of samples prepared at 500°C and those prepared at 900°C. The addition of potassium and low-temperature preparation increases the number of oxygen adsorbing sites. It also slightly decreases the characteristic heat of oxygen adsorption. Also, the heats show maxima and minima at low coverage, which is indicative of a nonequilibrium competition for adsorbate between sites of widely differing energetics (e.g., "carbon-type" and "potassium-type" adsorbing sites). In contrast on the high-temperature char the heats are remarkably low over a wide range of coverage. Also, the heat declines in an almost "stepped" fashion and the rate of adsorption is virtually constant over a broad coverage range. This suggests that equilibrium adsorption is taking place.

In sum, it is suggested that following high-temperature treatment the potassium is present as a thin film in a partially oxidized state, although it may be "complexed" with carbon. (It is felt that the same film has partially developed after the low-temperature treatment; however, it is clear the film has not fully developed after the low-temperature treatment. Also, after that treatment there are probably several different potassium species present.) Adsorption occurs initially in a kinetic and then in an equilibrium fashion until a well-defined stable oxide is formed (as per reaction (*6*)). This suggestion is in accord with the catalytic oxidation/reduction mechanism for CO_2 gasification proposed earlier by Moulijn and Kapteijn (*8, 10*).

Finally, a thin partially oxidized potassium layer suggests a mechanism for "activated oxygen" diffusion. That is, activated oxygen in the surface would need only to diffuse through one or two layers of catalyst to encounter carbon, at which interface catalyst reduction would take place. Thus, all potassium, not just that near particle edges, should be active. This is consistent with the finding that at low to moderate loading activity is proportional to the amount of potassium present on the char (*12*).

REFERENCES

1. Wen, W. Y., *Catal. Rev.-Sci. Eng.* **22,** 1 (1980).

2. Wood, B. J., and Sancier, K. M., *Catal. Rev.-Sci. Eng.* **26,** 233 (1984).

3. Walker, P. L., Jr., Shelef, M., and Anderson, R. A., *in* "Chemistry and Physics of Carbon" (P. L. Walker, Jr., Ed.), Vol. 4, pp. 287–383. Dekker, New York, 1968.

4. McKee, D. W., and Chatterji, D., *Carbon* **16,** 53 (1978).

5. Veraa, M. J., and Bell, A. T., *Fuel* **57,** 194 (1978).

6. Radovic, L. R., and Walker, Jr., P. L., *Fuel Process. Technol.* **8,** 149 (1984).

7. McKee, D. W., and Chatterji, D., *Carbon* **13,** 381 (1975).

8. Moulijn, J. A., and Kapteijn, F., "Carbon and Coal Gasification" (J. L. Figueiredo and J. A. Moulijn, Eds.), NATO ASI Series, Series E: Applied Sciences, No. 105, pp. 181–195. Martinus Nijhoff Publishers, Dordrecht, 1986.

9. Long, F. J., and Sykes, K. W., *Proc. Royal Soc.* London *Ser. A* **215,** 100 (1952).

10. Kapteijn, F., and Moulijn, J. A., *Fuel* **62,** 221 (1983).

11. McKee, D. W., *Fuel* **62,** 170 (1983).

12. Mims, C. A., and Pabst, J. K., *Fuel* **62,** 177 (1983).

13. Radovic, L. R., Walker, P. L., Jr., and Jenkins, R. G., *Fuel* **62,** 849 (1983).

14. Mahajan, O. P., and Walker, P. L., Jr., *Fuel* **58,** 333 (1979).

15. Mahajan, O. P. and Walker, P. L., Jr., *in* "Analytical Methods for Coal and Coal Products" (C. Karr, Ed.), Vol. 1, p. 125. Academic Press, New York, 1978.

16. Feates, F. S., Harris, P. S., and Reuben, B. G., *J. Chem. Soc. Faraday Trans. 1* **70,** 2011 (1974).

17. Dogen, G., and Ertl, G., *Surf. Sci.* **43,** 197 (1974).

18. Garcia, X., and Radovic, L. R., *Fuel* **65,** 292 (1986).

19. O'Neil, M., Lovrien, R., and Phillips, J., *Rev. Sci. Instrum.* **56,** 2312 (1985).

20. O'Neil, M., and Phillips, J., *J. Phys. Chem.* **91,** 2867 (1987).

21. Gatte, R. R., and Phillips, J., *Langmuir* **5,** 758 (1989).

22. Gatte, R. R., and Phillips, J., *J. Catal.* **116,** 49 (1989).

23. Laine, N. R., Vastola, F. J., and Walker, P. L., Jr., *J. Phys. Chem.* **67,** 2030 (1963).

24. Tucker, B. G., and Mulcahy, M. F. R., *Trans. Faraday Soc.* **65,** 274 (1969).

25. Bull, H. I., Hall, M. H., and Garner, W. E., *J. Chem. Soc.* **837** (1931).

26. Marshall, M. J., and MacInnes, A. S., *J. Can. Chem. Soc.* **75** (1937).

27. Keyes, F. G., and Marshall, M. J., *J. Am. Chem. Soc.* **49,** 156 (1927).

28. Bishop, M., and Ward, D. L., *Fuel* **37,** 191 (1958).

29. Walker, P. L., Jr., Matsumoto, S., Hanzawa, T., Muira, T., and Ismail, I. M. K., *Fuel* **62,** 140 (1983).

30. Mims, C. A., and Pabst, J. K., *Am. Chem. Soc. Fuel Chem. Div. Prepr.* **25,** 258 (1980).

31. Gow, A. S., and Phillips, J., *Thermochim. Acta* **148,** 173 (1989).

32. Wu, N. L., and Phillips, J., *Surf. Sci.* **184,** 463 (1987).

33. Lizzio, A. A., Jiang, H., and Radovic, L. R., *Carbon* **28,** 7 (1990).

34. Ehrlich, G. J., *J. Chem. Phys.* **36,** 1171 (1962).

35. Hickmott, T. W., and Ehrlich, G., *J. Phys. Chem. Solids* **5,** 47 (1958).

36. Otto, K., Bartosiewicz, L., and Shelef, M., *Fuel* **58,** 565 (1979).

37. Radovic, L. R., Walker, P. L., Jr., and Jenkins, R. G. *Fuel* **62,** 209 (1983).

38. Lang, R. J., and Neavel, R. C., *Fuel* **61,** 620 (1982).

39. Otto, K., Bartosiewicz, L., and Shelef, M., *Fuel* **58,** 85 (1979).

40. Spiro, C. L., McKee, D. W., Kosky, P. G., and E. J. Lamby, *Fuel* **63,** 686 (1984).

41. Mims, C. A., Chludzinski, J. J., Jr., Pabst, J. K., and Baker, R. T. K., *J. Catal.* **88,** 97 (1984).

42. Kuhn, L., and Plogmann, H., *Fuel* **62,** 205 (1983).

43. Kapteijn, F., Jurrians, J., and Moulijn, J. A., *Fuel* **62,** 249 (1983).

44. Mims, C. A., and Pabst, J. K., *in* "Proceedings of the International Conference on Coal Science," p. 730. Verlag Gluckauf GmbH, Essen, 1981.